Journal of Innovative Optical Health Sciences
Vol. 6, No. 1 (2013) 1330002 (9 pages)

DOI: 10.1142/S1793545813300024

World Scientific
www.worldscientific.com

SINGLET OXYGEN DETECTION DURING PHOTOSENSITIZATION*

BUHONG LI[†,¶], HUIYUN LIN[†], DEFU CHEN[‡],
BRIAN C. WILSON[§] and YING GU[‡]
[†]*Key Laboratory of OptoElectronic Science and Technology for Medicine of Ministry of Education*
Fujian Provincial Key Laboratory for Photonics Technology
Fujian Normal University, Fujian 350007, P. R. China
[‡]*Department of Laser Medicine*
Chinese PLA General Hospital, Beijing 100853, P. R. China
[§]*Department of Medical Biophysics*
University of Toronto, Ontario Cancer Institute, Toronto
Ontario M5G 2M9, Canada
[¶]*bhli@fjnu.edu.cm*

Received 18 October 2012
Accepted 22 November 2012
Published 31 January 2013

Singlet oxygen ($^1O_2$) is a highly reactive oxygen species involved in numerous chemical and photochemical reactions in different biological systems and in particular, in photodynamic therapy (PDT). However, the quantification of $^1O_2$ generation during *in vitro* and *in vivo* photosensitization is still technically challenging. To address this problem, indirect and direct methods for $^1O_2$ detection have been intensively studied. This review presents the available methods currently in use or under development for detecting and quantifying $^1O_2$ generation during photosensitization. The advantages and limitations of each method will be presented. Moreover, the future trends in developing PDT-$^1O_2$ dosimetry will be briefly discussed.

Keywords: Photodynamic therapy; photosensitization; singlet oxygen; detection; probe; luminescence.

1. Introduction

Photodynamic therapy (PDT) is an emerging treatment modality that uses a light source to activate light-sensitive photosensitizer (PS) to treat cancer and other diseases, such as age-related macular degeneration, port-wine stain and localized infection.[1,2] As the basic research and clinical applications of PDT continue to develop, a robust individualized

*An earlier version of this paper was presented at the 13th International Photodynamic Association World Congress, Innsbruck, Austria, May 11−14, 2011.
¶Corresponding author.

dosimetry is vital for achieving satisfactory outcomes, which still remains a challenge to be solved in clinics.[3,4] The essential effector in Type-II PDT is believed to be singlet oxygen ($^1O_2$), and its concentration or amount is the direct indicator of clinical PDT dosimetry.[3,5] As a result, the detection and quantification of $^1O_2$ generation correlated to the efficacy during PDT treatment has received considerable attention, which also play an important role in the elucidation of biological mechanisms.[6–9] As compared to the implicit and explicit dosimetry, the most attractive advantage of direct PDT-$^1O_2$ dosimetry is that it can circumvent the complicated interactions between the PS, irradiation light, and molecular oxygen. This paper reviews the available methods currently in use or under development for detecting and quantifying $^1O_2$ generation and presents the advantages and limitations of each method. Moreover, the future trends in developing PDT-$^1O_2$ dosimetry will be briefly discussed.

2. $^1O_2$ Detection Methods

As shown in Fig. 1, the ground state (S_0) of PS absorbs the photon energy and is excited to an excited state (S_1), which can de-excite either by fluorescence emission or by intersystem crossing (ISC) to a triplet state (T_1). The transition from T_1 to S_0 is quantum-mechanically forbidden, but T_1 can exchange energy with ground state molecular oxygen ($^3O_2$) to generate cytotoxic $^1O_2$. Once generated, $^1O_2$ can undergo non-radiative decay, oxidize surrounding biomolecules, or undergo radiative decay at about 1270 nm. To date, it is believed that the majority of approved and studied photosensitizers in PDT elicit their damage primarily through $^1O_2$-mediated pathways.

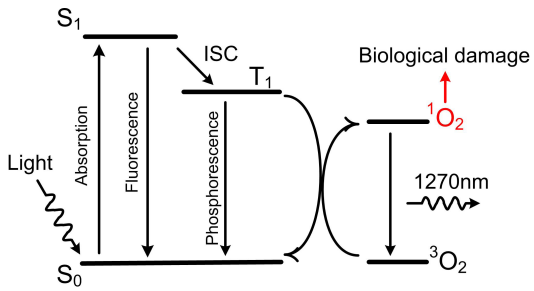

Fig. 1. Simplified Jablonski energy-level diagram for Type-II ($^1O_2$ mediated) PDT. During photosensitization, $^1O_2$ is widely regarded as the major cytotoxic reactive oxygen species that resulted in biological damage.

Although the direct detection of near-infrared (NIR) luminescence around 1270 nm is the gold standard for $^1O_2$ identification, this method remains technically challenging in biological systems due to the extremely weak emission that results from the very high reactivity of $^1O_2$, of which only about one in 10^8 $^1O_2$ molecules undergoes luminescence deactivation. For this, the indirect detection methods using the electron paramagnetic resonance (EPR), absorption, fluorescence, and chemiluminescence (CL) probe have been developed. Meanwhile, the detection of $^1O_2$ generation can be performed in non-imaging and imaging modalities in order to obtain the spectral information and spatial distribution, respectively.

2.1. *Indirect methods*

Spectrophotometry is the most convenient method for $^1O_2$ detection, and $^1O_2$ can be indirectly detected via EPR, absorption, fluorescence, or CL by adding the commercial $^1O_2$ probes, such as 2,2,6,6-tetramethylpiperidine (TEMP, Sigma Aldrich, St. Louis, MO, USA), 1,3-Diphenylisobenzofuran (DPBF, Sigma Aldrich, St. Louis, MO, USA), Singlet Oxygen Sensor Green (SOSG, Molecular Probes, Eugene, OR, USA) and fluoresceinyl cypridina luciferin analogue (FCLA, Tokyo Kasei Kogyo Co., Tokyo, Japan).[10–15] Among these probes, fluorescence probes with high sensitivity hold great potential for $^1O_2$ detection with a conventional photomultiplier tube (PMT), and the limitations for other chemical probes will be discussed thereafter.

2.1.1. *Indirect spectroscopic detection of $^1O_2$ generation*

As a fluorescence probe model, SOSG became commercially available in 2004. In the presence of $^1O_2$, SOSG can react with $^1O_2$ to produce SOSG endoperoxides (SOSG-EP) that emit strong green fluorescence with the maximal peak at 531 nm. $^1O_2$ generation from the irradiation of Rose Bengal (RB) in phosphate buffered saline (PBS) can be readily monitored by using SOSG as a fluorescence probe. Figure 2(a) shows the fluorescence emission spectra from RB itself, SOSG and a mixture of RB + SOSG at equimolar concentrations, before and after photoirradiation. RB has a maximum fluorescence emission peak at 565 nm, while its emission at 531 nm is negligible compared to that of SOSG.

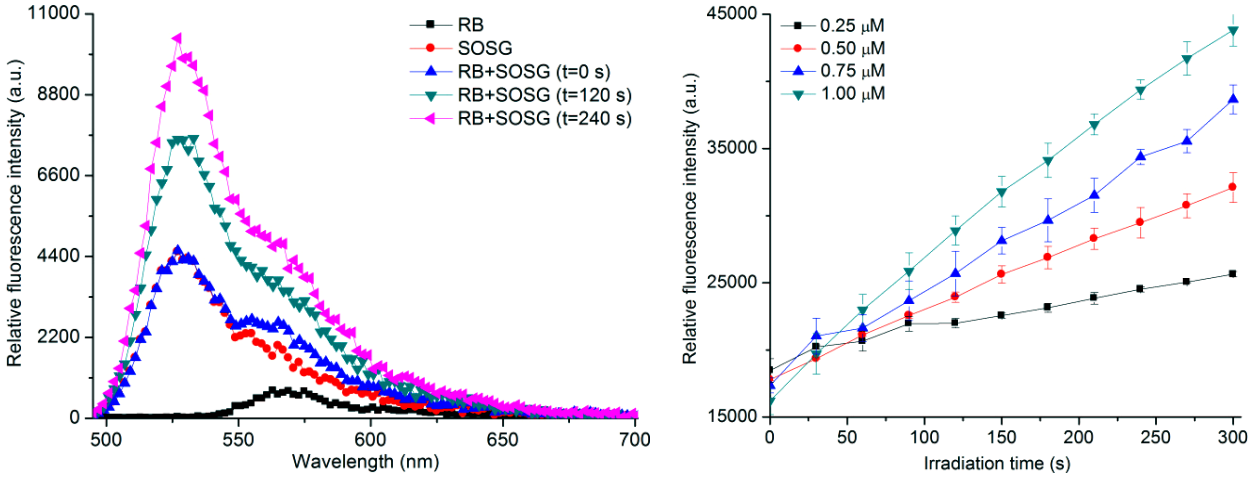

(a) (b)

Fig. 2. (a) Fluorescence emission spectra of 1.00 μM RB and 1.00 μM SOSG before irradiation and a mixture of RB+SOSG before and at two different time points after irradiation. (b) Reaction of 6.00 μM SOSG with $^1O_2$ generation from various concentrations of RB. Fluorescence excited at 488 nm.

Upon irradiation, the green fluorescence intensity in the mixture solution of RB + SOSG continuously increased with the irradiation time, representing the generation of $^1O_2$ during the irradiation and much higher fluorescence of SOSG-EP compared to SOSG. Furthermore, the zeroth-order reactions for 6.00 μM SOSG reacting with $^1O_2$ that generated from RB photosensitization were studied. Figure 2 (b) shows the reaction kinetic curves (curve slope, which is paralleling the formation rate of SOSG-EP). The slope increases with the increase of RB concentration. This study demonstrates that the quantitative measurement of $^1O_2$ generation using SOSG can be achieved by determining the initial reaction rates with an appropriate measurement protocol.[16]

2.1.2. *Indirect imaging of $^1O_2$ generation*

Indirect imaging of $^1O_2$ generation from the polymeric nanofiber materials loaded with tetraphenylporphyrin was successfully visualized by the $^1O_2$-sensitized delayed fluorescence imaging (SODF).[17] Meanwhile, $^1O_2$ generation from the plasma membrane-targeted protoporphyrin IX (PpIX) and nuclear-targeted meso-Tetra (N-methyl-4-pyridyl) porphine tetra tosylate (TMPyP) in human nasopharyngeal carcinoma CNE2 cells can be indirectly imaged and analyzed by using the fluorescence probe SOSG, respectively. As shown in Fig. 3, the confocal images indicate that the green fluorescence of SOSG in the vicinity of the PpIX-sensitized cells was dramatically enhanced with the increase of the irradiation time and intracellular PpIX, while there was no significant enhancement for the TMPyP-sensitized cells. Our study suggests that the $^1O_2$ generated from the plasma membrane-targeted PpIX in the CNE2 cells can escape into the extracellular medium and react with the SOSG to produce SOSG-EP, but the $^1O_2$ generated in the nucleus cannot. This is the first study that demonstrates the $^1O_2$ generation inside the intact cells cannot diffuse a great distance from its site of generation.[18]

2.2. *Direct methods*

Measurement of $^1O_2$ luminescence during photosensitization in air-saturated solutions provided the development of direct method for kinetic analysis of photodynamic reactions, and the $^1O_2$ luminescence can be detected without addition of chemical probes.[8,19] A NIR photodetector, FEU-83 PMT cooled to -60° C with S-1 spectral response was successfully used for the direct detection of $^1O_2$ luminescence in 1976.[20] With the development of high-sensitive NIR-PMT (R5509 and H10330; Hamamatsu Corp., Hamamatsu, Japan), NIR-camera (Xeva-1.7-320, Xenics, Leuven, Belgium and MOSIR 950, Intevac, Inc., CA, USA), pulse laser with short duration and high repetition rates,

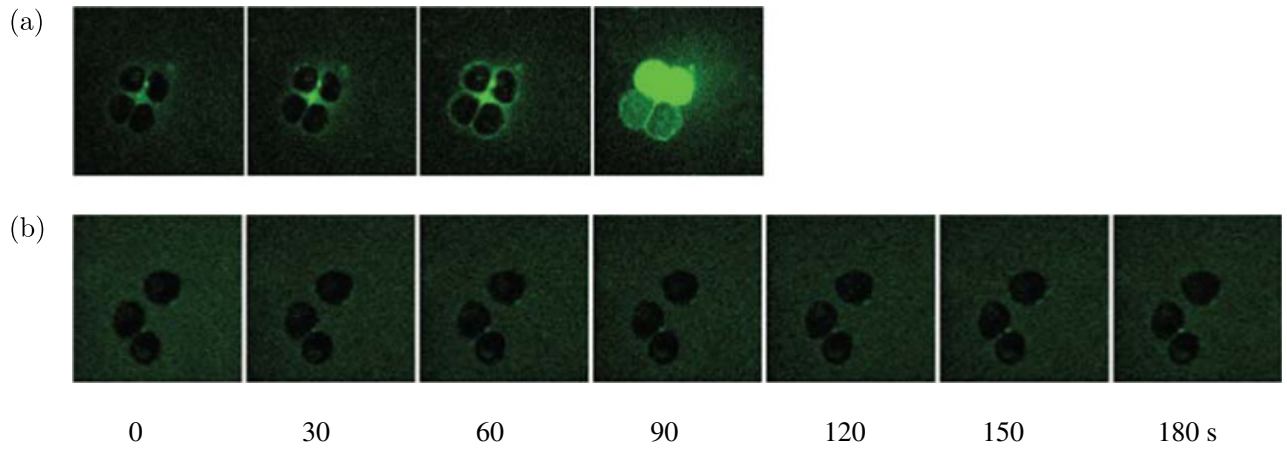

Fig. 3. CNE2 cells were incubated with: (a) 4 μM PpIX for 1 h and (b) 100 μM TMPyP for 6 h, respectively. The confocal images of SOSG were acquired at various time points after continuous irradiation with 633 nm laser.

and the single photon counter (MSA-300; Becker and Hickl GmbH, Berlin, Germany), the most common temporal and spectral-resolved detection systems for $^1O_2$ luminescence measurement have been developed worldwide for determining the $^1O_2$ lifetimes and quantum yields in solution, cells (*in vitro*) and tissues (*in vivo*).[21–27]

2.2.1. *Temporal and spectral-resolved detection of $^1O_2$ luminescence*

In order to improve the signal-to-noise ratio (SNR), the systems that combined temporal-resolved with spectral-resolved measurement were developed for $^1O_2$ luminescence detection since the spectral resolution alone usually cannot be sufficient to discriminate the $^1O_2$ luminescence from other background sources, which includes PS fluorescence and phosphorescence, fluorescence and scattering light from the optical detection system. The representative temporal and spectral-resolved $^1O_2$ luminescence detection system is shown schematically in Fig. 4.[26]

Laser at 523 nm from a diode-pumped, Q-switched, frequency-doubled Nd:YLF laser (QG-523-500; Crystalaser Inc., Reno, NV, USA) was used as the excitation light source. The sample is excited by the laser and the $^1O_2$ luminescence signal is detected by a PMT (H10330-45; Hamamatsu Corp., Hamamatsu, Japan) in the photon counting mode. The PMT pulses are recorded by a fast photon counter (MSA-300; Becker and Hickl GmbH, Berlin, Germany), which is triggered from the reflection laser by a photodiode (PDM-400; Becker and Hickl GmbH, Berlin, Germany). A 1000 nm long-pass filter (Omega Optical, Brattleboro, VT, USA) was used to block out the unwanted scattering excitation light and fluorescence from the sample. The collected NIR luminescence reaches the PMT photocathode through a custom designed optical collected unit. The PMT is contained in a thermally insulated sealed-off housing evacuated to a high vacuum, and the internal thermoelectric cooler eliminated the need for liquid nitrogen and cooling water. The operating voltage of the PMT was set to −900 V. The PMT output was amplified using a high-speed wide-band pre-amplifier (HFAC-26; Becker and Hickl GmbH, Berlin, Germany). Spectral discrimination of the detected luminescence was achieved using a set of five narrow-band filters centered at 1190, 1230, 1270, 1310, and 1350 nm (OD6 blocking, 20 nm FWHM; Omega Optical, Brattleboro, VT, USA) mounted on a six-position motorized filter wheel (FW102B; Thorlabs Inc., Newton, NJ, USA) in front of the PMT. These filters allowed sampling of the NIR $^1O_2$ luminescence spectrum. The control panel software of the detection system is designed by LabVIEW 8.5 (National Instruments Corp. Austin, TX, USA), and operated on a personal computer (PC).

Figure 5(a) shows the temporal-resolved NIR luminescence of the five wavelengths for 8 μM RB in distilled water, and the $^1O_2$ luminescence at 1270 nm can be clearly identified. In order to remove the fast fluorescence and background of the detection system, the corresponding time-integrated spectra were generated by summing the delayed luminescence for the five individual wavelengths from 1 to 25 μs, respectively. As expected, a strong

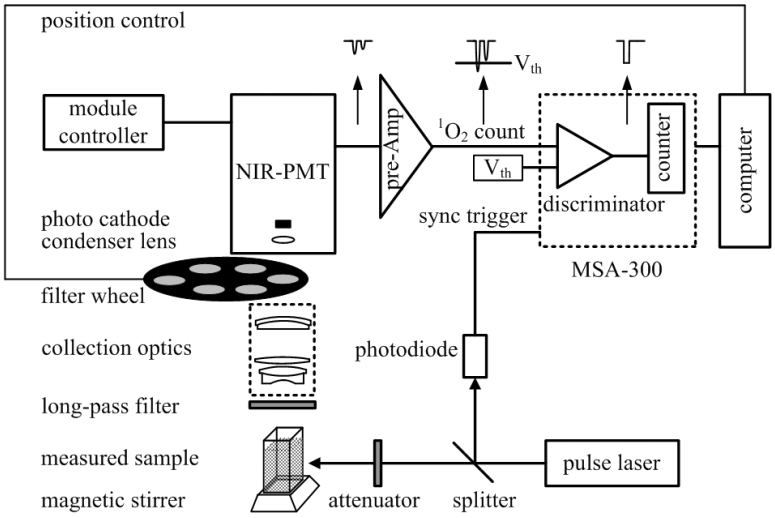

Fig. 4. Experimental setup of the temporal and spectral-resolved $^1O_2$ luminescence detection. The collection optics, detection configuration and electronics of the system are indicated.

spectral peak was observed at 1270 nm, as shown in Fig. 5(b). Furthermore, the $^1O_2$ luminescence intensity at 1270 nm was linearly dependent on RB concentration, as described in the inset of Fig. 5(b).

Recently, the influence of oxygen depletion and photosensitizer triplet-state dynamics during PDT on accurate $^1O_2$ monitoring and analysis of treatment dose response was quantitatively investigated.[28] Meanwhile, the influence of pulse-height discrimination threshold on measurement accuracy of the $^1O_2$ luminescence that generated from the photoirradiation of TMPyP in aqueous solution was quantitatively evaluated by using the above system that developed in our lab.[29] The obtained results indicate that the discrimination threshold not only has a significant influence on the absolute $^1O_2$ luminescence counts, but also on the shape of the time-resolved $^1O_2$ luminescence, which resulted in a poor goodness-of-fit that required to determine the PS triplet-state and $^1O_2$ lifetimes. Most recently, Sackbarth *et al.* observed a strong dependency of the $^1O_2$ luminescence kinetics from the applied illumination at very low doses for two cell lines incubated with three different photosensitizers.[30]

2.2.2. *Direct imaging of $^1O_2$ luminescence*

In this method, InGaAs linear array detector, NIR-PMTs and NIR-cameras were used to obtain the spatial-resolution of $^1O_2$ luminescence. Ogilby's

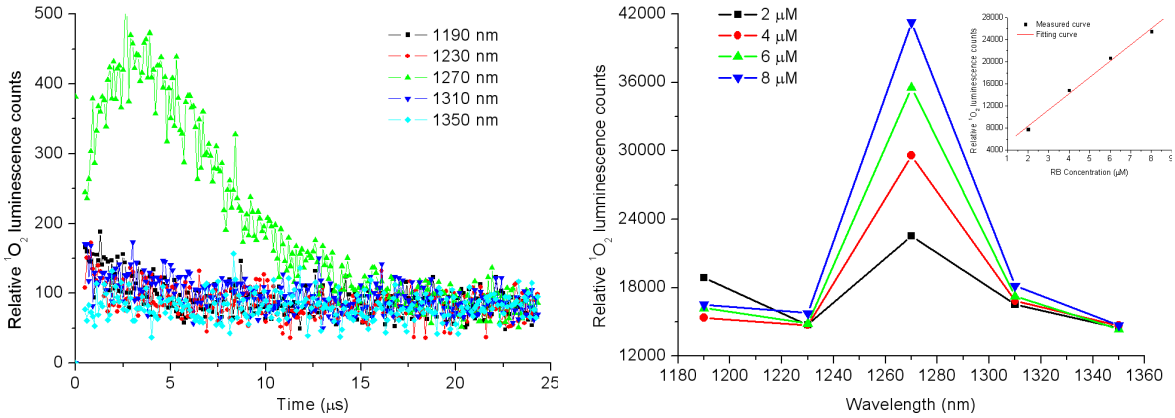

(a) (b)

Fig. 5. (a) Temporal- and (b) spectral-resolved $^1O_2$ luminescence for RB in distilled water.

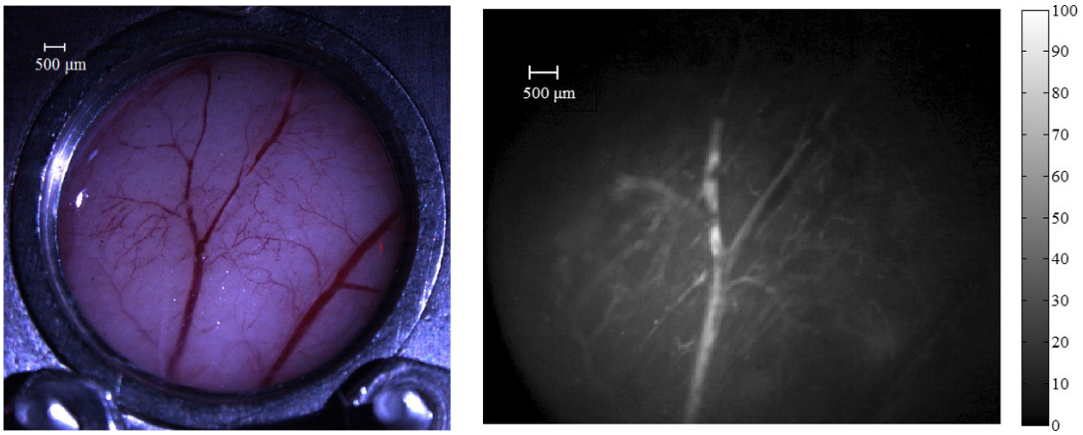

(a) (b)

Fig. 6. (a) White-light and (b) $^1O_2$ luminescence images for the blood vessels within a rodent dorsal window chamber model.

group used an InGaAs linear array detector to construct an imaging system, and the $^1O_2$ luminescence images of a single cell was obtained with a spatial resolution of 2.5 μm.[31–33] Niedre *et al.* obtained a $^1O_2$ luminescence image from an intradermal tumor model in mice by a laser-scanning system with NIR-PMT.[34] Recently, Hu *et al.* reported the images of $^1O_2$ luminescence from the tumor-bearing nude mouse with intravenous injection of BPD-MA by using a cooled NIR-camera, and they showed the real-time $^1O_2$ signal depletion as a function of the light exposure.[35] Lee *et al.* developed a two-channel optical system to provide spatially resolved simultaneous imaging of $^1O_2$ luminescence and PS fluorescence generated during photosensitization, and the preliminary images with tumor-laden mice indicate that it is possible to obtain simultaneous images of $^1O_2$ and PS distribution.[36] Most recently, we also have developed an imaging system for $^1O_2$ luminescence with a cooled NIR-camera. As shown in Fig. 6, the $^1O_2$ luminescence image of blood vessels after background subtraction with a resolution of 30 μm and with a maximal area of $9.60 \times 7.68\,mm^2$ was acquired, and the details of which will be published elsewhere.

3. Advantages and Limitations of Each Detection Method for $^1O_2$ Generation

The advantages and limitations of the currently available methods for $^1O_2$ detection are summarized in Table 1. Compared to the direct methods, the indirect measurement of $^1O_2$ with the specific probe, in particular, the newly developed multifunctional fluorescence probe, has the advantage of very high sensitivity, which has great potential for $^1O_2$ detection. However, the enhanced fluorescence of the probe may not exactly reflect the amount of generated $^1O_2$ because the localization of the probe may differ from the $^1O_2$ generation site during photosensitization. In addition, the chemical reaction will unavoidably consume the desired cytotoxic $^1O_2$ for PDT. Therefore, substantial improvements for analytical characteristics of the developed $^1O_2$ fluorescence probes are needed to achieve the accurate measurement. The direct measurement of $^1O_2$ with its luminescence has three main advantages: the detection is non-invasive and can be performed in real-time and the information of the $^1O_2$ lifetime and ^{3}PS lifetime can be provided simultaneously. However, this method is technically challenging due to the extremely low efficiency for $^1O_2$ emission and the low quantum yield of the available NIR photodetector, which is also accompanied by the strong scattered light in biological environments. Hopefully, these limitations will be effectively overcome by newly developed PS with enhanced $^1O_2$ radiative transition as well as new InGaAs photodiode with higher quantum efficiency.

4. Conclusions

To date, although the direct detection methods of $^1O_2$ generation are predictive of PDT responses both *in vitro* and *in vivo*, the accurate quantification and absolute comparison are still technically

Table 1. Advantages and limitations of the currently available methods for $^1O_2$ detection.

Detection methods			Advantages		Limitations	
Indirect	**Spectroscopy**	Absorption probe	Easy detection Convenient usage		$^1O_2$ consumption Potential cytotoxicity Microenvironment dependent	Poor photostability Low sensitivity
		Fluorescence probe	Easy detection High sensitivity	Fast response Good specificity		Act as a PS itself
		CL probe		High SNR		Poor water solubility Non-specificity Delay measurement
		EPR probe	High sensitivity Good selectivity			High cost Complicated operation
	Imaging	Fluorescence probe	High sensitivity	Easy detection		Act as a PS itself
		Delay fluorescence		Non-invasive	Limited to specific drug delivery system	
Direct	**Spectroscopy**	NIR luminescence at 1270 nm	Non-invasive Real-time	Providing information about the $^1O_2$ lifetime and ^{3}PS lifetime	Extremely low emission efficiency Low sensitivity and SNR High cost	Low quantum yield of NIR detector
	Imaging			Spatial distribution		Limited area

challenging. As illustrated in Fig. 7, in order to establish the direct robust PDT-$^1O_2$ dosimetry, the following perspectives are important for future studies. First, the mechanisms for how PS dose and photobleaching, light dose, oxygen concentration and the targeted tissue optical properties influence the amount of $^1O_2$ generation during PDT should be quantitatively investigated for optimizing and adjusting treatment protocols for clinical applications. Second, the detection system for time-resolved $^1O_2$ luminescence may be integrated with the $^1O_2$ luminescence imaging system, which allows us simultaneously to obtain not only the temporal information but also the spatial distribution of $^1O_2$ generation during PDT. In addition, more sophisticated theoretical models are needed in order to interpret the kinetics of $^1O_2$ luminescence. Finally, for different $^1O_2$ detection systems, the determined concentration or amount for $^1O_2$ generation should be comparable for establishing robust PDT-$^1O_2$ dosimetry.

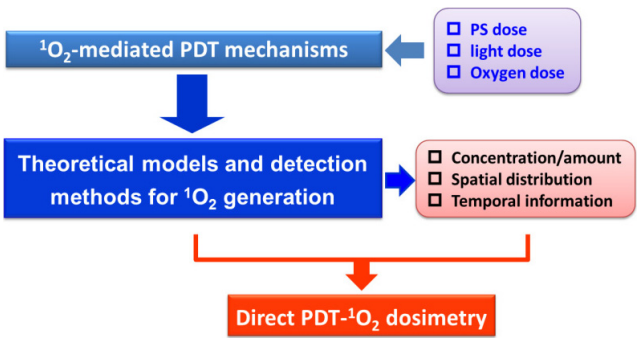

Fig. 7. Future trends in developing PDT-$^1O_2$ dosimetry.

Acknowledgments

This study was supported by the National Natural Science Foundation of China (60978070, 61036014, 61175216), the Natural Science Foundation for Distinguished Young Scholars of Fujian Province (2011J06022), the program for New Century Excellent Talents in University of China (NCET-10-0012), and the Program for Changjiang Scholars and Innovative Research Team in University (IRT1115).

References

1. J. P. Celli, B. Q. Spring, I. Rizvi *et al.*, "Imaging and photodynamic therapy: Mechanisms, monitoring, and optimization," *Chem. Rev.* **110**(5), 2795 (2010).
2. P. Agostinis, K. Berg, K. A. Cengel *et al.*, "Photodynamic therapy of cancer: An update," *CA. Cancer J. Clin.* **61**(4), 250 (2011).
3. M. T. Jarvi, M. J. Niedre, M. S. Patterson *et al.*, "Singlet oxygen luminescence dosimetry (SOLD) for photodynamic therapy: Current status, challenges and future prospects," *Photochem. Photobiol.* **82**(5), 1198 (2006).
4. B. Li, S. Xie, Z. Huang *et al.*, "Advances in photodynamic therapy dosimetry," *Prog. Biochem. Biophys.* **36**(6), 676 (2009).
5. K. R. Weishaupt, C. J. Gomer, T. J. Dougherty, "Identification of singlet oxygen as the cytotoxic agent in photoinactivation of a murine tumor," *Cancer Res.* **36**(7), 2326 (1976).

6. P. R. Ogilby, "Singlet oxygen: There is indeed something new under the sun," *Chem. Soc. Rev.* **39**(8), 3181 (2010).
7. J. R. Kanofsky, "Measurement of singlet-oxygen *in vivo*: Progress and pitfalls," *Photochem. Photobiol.* **87**(1), 14 (2011).
8. B. Li, B. C. Wilson, "Direct and indirect measurements of singlet oxygen for photodynamic therapy," *Proc. 13th Int. Photodynamic Assoc. World Congress*, pp. 43−47 (2011).
9. V. Vyklický, R. Dědic, N. Curkaniuk *et al.*, "Spectral- and time-resolved phosphorescence of photosensitizers and singlet oxygen: From *in vitro* towards *in vivo*," *J. Lumin.* doi:10.1016/j.jlumin.2011.12.033 (2011).
10. H. Wu, Q. Song, G. Ran *et al.*, "Recent developments in the detection of singlet oxygen with molecular spectroscopic methods," *Trend. Anal. Chem.* **30**(1), 133 (2011).
11. C. Hadjur, G. Wagnieres, P. Monnier *et al.*, "EPR and spectrophotometric studies of free radicals ($O_2^{\circ}-$, °OH, BPD-MA°−) and singlet oxygen ($^1O_2$) generated by irradiation of benzoporphyrin derivative monoacid ring A," *Photochem. Photobiol.* **65**(5), 818 (1997).
12. Y. Wei, J. Zhou, D. Xing *et al.*, "*In vivo* monitoring of singlet oxygen using delayed chemiluminescence during photodynamic therapy," *J. Biomed. Opt.* **12**(1), 014002 (2007).
13. A. Gollmer, J. Arnbjerg, F. H. Blaikie *et al.*, "Singlet Oxygen Sensor Green®: Photochemical behavior in solution and in a mammalian cell," *Photochem. Photobiol.* **87**(3), 671 (2011).
14. B. R. Rabello, A. P. Gerola, D. S. Pellosi *et al.*, "Singlet oxygen dosimetry using uric acid as a chemical probe: Systematic evaluation," *J. Photochem. Photobiol. A* **238**, 53 (2012).
15. D. Kessel, M. Price, "Evaluation of diethyl-3-3′-(9,10-anthracenediyl)bis acrylate as a probe for singlet oxygen formation during photodynamic therapy," *Photochem. Photobiol.* **88**(3), 717 (2012).
16. H. Lin, Y. Shen, D. Chen *et al.*, "Feasibility study on quantitative measurements of singlet oxygen generation using Singlet Oxygen Sensor Green," *J. Fluoresc.* doi: 10.1007/s10895-012-1114-5 (2012).
17. J. Mosinger, K. Lang, J. Hostomsky *et al.*, "Singlet oxygen imaging in polymeric nanofibers by delayed fluorescence," *J. Phys. Chem. B* **114**(48), 15773 (2010).
18. Y. Shen, H. Lin, Z. Huang *et al.*, "Indirect imaging of singlet oxygen generation from a single cell," *Laser Phys. Lett.* **8**(3), 232 (2011).
19. A. A. Krasnovsky Jr., "Luminescence and photochemical studies of singlet oxygen photonics," *J. Photochem. Photobiol. A* **196**(2−3), 210 (2008).
20. A. A. Krasnovsky Jr., "Photosensitized luminescence of singlet oxygen in solution," *Biofizika* **21**(4), 748 (1976).
21. M. Niedre, M. S. Patterson, B. C. Wilson, "Direct near-infrared luminescence detection of singlet oxygen generated by photodynamic therapy in cells *in vitro* and tissues *in vivo*," *Photochem. Photobiol.* **75**(4), 382 (2002).
22. J. Baier, T. Maisch, M. Maier *et al.*, "Singlet oxygen generation by UVA light exposure of endogenous photosensitizers," *Biophys. J.* **91**(4), 1452 (2006).
23. J. Yamamoto, S. Yamamoto, T. Hirano *et al.*, "Monitoring of singlet oxygen is useful for predicting the photodynamic effects in the treatment for experimental glioma," *Clin. Cancer Res.* **12**(23), 7132 (2006).
24. A. Jimenez-Banzo, X. Ragas, P. Kapusta *et al.*, "Time-resolved methods in biophysics. 7. Photon counting vs. analog time-resolved singlet oxygen phosphorescence detection," *Photochem. Photobiol. Sci.* **7**(9), 1003 (2008).
25. J. Schlothauer, S. Hackbarth, B. Roder, "A new benchmark for time-resolved detection of singlet oxygen luminescence — Revealing the evolution of lifetime in living cells with low dose illumination," *Laser Phys. Lett.* **6**(3), 216 (2009).
26. B. Li, H. Lin, D. Chen *et al.*, "Detection system for singlet oxygen luminescence in photodynamic therapy," *Chin. Opt. Lett.* **8**(1), 86 (2010).
27. W. Baumler, J. Regensburger, A. Knak *et al.*, "UVA and endogenous photosensitizers — The detection of singlet oxygen by its luminescence," *Photochem. Photobiol. Sci.* **11**(1), 107 (2012).
28. M. T. Jarvi, M. J. Niedre, M. S. Patterson *et al.*, "The influence of oxygen depletion and photosensitizer triplet-state dynamics during photodynamic therapy on accurate singlet oxygen luminescence monitoring and analysis of treatment dose response," *Photochem. Photobiol.* **87**(1), 223 (2011).
29. H. Lin, D. Chen, M. Wang *et al.*, "Influence of pulse-height discrimination threshold for photon counting on the accuracy of singlet oxygen luminescence measurement," *J. Opt.* **13**(12), 125301 (2011).
30. S. Hackbarth, J. Schlothauer, A. Preuss *et al.*, "Time-resolved sub-cellular singlet oxygen detection-ensemble measurements versus single cell experiments," *Laser Phys. Lett.* **9**(6), 474 (2012).
31. L. K. Andersen, Z. Gao, P. R. Ogilby *et al.*, "A singlet oxygen image with 2.5 μm resolution," *J. Phys. Chem. A.* **106**(37), 8488 (2002).
32. I. Zebger, J. W. Snyder, L. K. Andersen *et al.*, "Direct optical detection of singlet oxygen from a single cell," *Photochem. Photobiol.* **79**(4), 319 (2004).

33. J. W. Snyder, E. Skovsen, J. D. Lambert *et al.*, "Sub-cellular, time-resolved studies of singlet oxygen in single cells," *J. Amer. Chem. Soc.* **127**(42), 14558 (2005).
34. M. J. Niedre, M. S. Patterson, A. Giles *et al.*, "Imaging of photodynamically generated singlet oxygen luminescence *in vivo*," *Photochem. Photobiol.* **81**(4), 941 (2005).
35. B. Hu, N. Zeng, Z. Liu *et al.*, "Two-dimensional singlet oxygen imaging with its near-infrared luminescence during photosensitization," *J. Biomed. Opt.* **16**(1), 016003 (2011).
36. S. Lee, M. E. Isabelle, K. L. Gabally-Kinney *et al.*, "Dual-channel imaging system for singlet oxygen and photosensitizer for PDT," *Biomed. Opt. Express* **2**(5), 1233 (2011).